

Gradual disaggregation of the casein micelle improves its emulsifying capacity and decreases the stability of dairy emulsions

Fanny Lazzaro^{a, b}, Arnaud Saint-Jalmes^c, Frédéric Violleau^d, Christelle Lopez^a, Mireille Gaucher-Delmas^e, Marie-Noëlle Madec^a, Eric Beaucher^a, Frédéric Gaucheron^{a, *}

^a STLO, Agrocampus Ouest, INRA, 35000, Rennes, France

^b CNIEL, Paris, France

^c Institut de Physique de Rennes, UMR 6251, CNRS-Université Rennes 1, Rennes, France

^d Laboratoire de Chimie Agro-Industrielle (LCA), Université de Toulouse, INRA, INPT, INP-EI PURPAN, Toulouse, France

^e INP – Ecole d'Ingénieurs de PURPAN, Département Sciences Agronomique & Agroalimentaires, Université de Toulouse, Toulouse, France

ARTICLE INFO

Article history:

Received 4 May 2016

Received in revised form

22 August 2016

Accepted 26 August 2016

Available online 28 August 2016

Keywords:

Milk

Citrate

Mineral

Calcium phosphate

Functionality

Casein aggregate

ABSTRACT

The casein micelle is a highly aggregated colloid consisting of phosphoproteins and minerals, in particular calcium and phosphate. Its properties are affected by physico-chemical changes which provide possibilities for the development of new casein aggregates (CAs) with novel functionalities. The aim of this study was to investigate the emulsifying and emulsion-stabilizing capacity of gradually demineralized CAs in model dairy emulsions. Tri sodium citrate (TSC) was used to remove calcium and inorganic phosphate from pure casein micelles in order to produce four suspensions of differently demineralized CAs. Two types of milkfat-in-suspension (30:70 v/v) emulsions were then prepared to study the emulsifying and emulsion-stabilizing capacity of these CAs separately. Casein micelles were progressively demineralized (from 24 to 81% calcium reduction) and dissociated with the increase in TSC concentration. Three distinct populations of particles (micelle-like aggregates, sodium caseinate-like aggregates and casein monomers) were present in every suspension in different proportions. The smaller CAs had better emulsifying capacity and similar surface activity according to interfacial studies. The state of aggregation of the CAs was thus the main factor that controlled their emulsifying capacity. However, the emulsions formed with these smaller aggregates were less stable against creaming and flocculation, but still resisted coalescence under our storage conditions (21 days at 50 °C). The properties of the interfacial casein layers did not depend on the aggregation state of the CAs used to form the emulsions. The differences in instability were attributed to the nature of the non-adsorbed CAs and storage conditions.

© 2016 Elsevier Ltd. All rights reserved.

1. Introduction

The casein micelle consists of a highly aggregated particle of 150–200 nm diameter constituted of proteins (*i.e.* the four casein molecules α_{S1} , α_{S2} , β , κ), and minerals (mainly calcium phosphate) that ensure its colloidal stability (Dalglish & Corredig, 2012; Holt & Horne, 1996; Holt, Carver, Ecroyd, & Thorn, 2013; Marchin, Putaux, Pignon, & Léonil, 2007; Schmidt & Payens, 1976; Trejo, Dokland, Jurat-Fuentes, & Harte, 2011; Walstra, 1990). The casein micelle has a key role in food products, especially dairy products, as it often contributes to their functional properties (*i.e.* the ability to form

and/or stabilize networks such as gels, foams and emulsions, etc) (Foegeding & Davis, 2011).

The colloidal properties of the casein micelle (structure, composition, charge, hydration, etc) can be modified by controlling environmental factors such as pH, salt and chelating agent addition, temperature, etc (de Kort, Minor, Snoeren, van Hooijdonk, & van der Linden, 2011; Gaucheron, 2004; Silva et al., 2013). However, only a few studies have described the link between the colloidal organization and the functional properties of the modified casein micelle (Broyard & Gaucheron, 2015). Of all their functional properties, the capacity of the casein micelle to emulsify and stabilize oil in water emulsions is of great interest for the food industry, especially for the dairy industry. Indeed, many dairy products are edible emulsions (*e.g.* cream and ice-cream, infant formulae, etc) (Barbosa-Cánovas, Kokini, Ma, & Ibarz, 1996; Guzey & McClements,

* Corresponding author.

E-mail address: frederic.gaucheron@rennes.inra.fr (F. Gaucheron).

2006).

Emulsions consist of mixtures of two immiscible liquids (such as oil and water), one of the liquids being dispersed as droplets in the other (McClements, 2005). These systems are thermodynamically unstable. The two phases will separate as a result of creaming, flocculation (agglomeration) and/or coarsening (fusion by coalescence or Oswald ripening) of the droplets. It is crucial to control both their formation and their stability during manufacture and storage to ensure the final quality of food emulsions. One way to improve the formation and the stability of emulsions is to use emulsifying agents that adsorb at the oil-water interface and lower its tension. This results in the formation of smaller droplets that are less prone to creaming. The adsorbed layer formed by the emulsifying agents at the droplet surface can also protect the emulsion against flocculation and coalescence. Emulsifying agents can be assessed according to two main characteristics: their ability to facilitate the blending of the emulsion phases (*i.e.* emulsifying capacity) and their ability to stabilize the emulsion (*i.e.* emulsion-stabilizing capacity). Caseins are known to adsorb at the interface, either in individual or aggregated form (Dickinson, 1999), and are therefore able to fulfill the role of emulsifying agent.

The emulsifying and stabilizing capacity of caseins is associated with their chemical nature and conformation at the interface and also depend on their aggregation state. Poorly aggregated casein systems such as sodium caseinate (30–50 nm diameter – formed by extreme acid demineralization of native casein micelle) (Pitkowski, Durand, & Nicolai, 2008) have enhanced emulsifying properties but are less effective for the stabilization of emulsions than highly aggregated casein micelles (Courthaudon et al., 1999; Mulvihill & Murphy, 1991). However, little information is available on the emulsifying properties of the intermediate aggregation states of casein micelles. Ye (2011) contributed to this information by studying different milk protein concentrates (MPCs) containing both casein and whey proteins as well as lactose in soya oil-based emulsions. Demineralization of the MPCs was induced by cation exchange but did not control the diffusible phase.

The aim of our study was to investigate the effects of the gradual disaggregation of pure casein micelles on their colloidal properties and on their emulsifying and stabilizing capacity in model dairy emulsions. Tri sodium citrate (TSC), a calcium chelating salt, was used to remove calcium and inorganic phosphate from the casein micelle and to produce four suspensions of differently demineralized casein aggregates (CAs). Dialysis was performed on each suspension to control their diffusible phases. The CAs in these suspensions were characterized physico-chemically and used to form two types of emulsion to study their emulsifying and emulsion-stabilizing capacity separately. In addition, emulsions containing large droplets were produced to facilitate the creaming during storage and foster the appearance of flocculation and coalescence.

2. Materials and methods

2.1. Chemicals

All chemicals used for this study, hydrochloric acid (HCl) and tri sodium citrate (TSC) (Carlo Erba reagent, Val de Reuil, France), sodium azide (NaN_3) (Riedel-de Haën, Seelze, Germany), sodium hydroxide (NaOH), sodium dodecyl sulfate (SDS), D(+)-saccharose (saccharose) (VWR international, Leuven, Belgium), calcium chloride dihydrate ($\text{CaCl}_2 \cdot 2\text{H}_2\text{O}$) (Sigma-Aldrich, St. Louis, USA), sodium di-hydrogen phosphate 2-hydrate ($\text{NaH}_2\text{PO}_4 \cdot 2\text{H}_2\text{O}$) (Panreac, Barcelona, Spain), Fast Green FCF (FG) (Sigma-Aldrich, St. Louis, USA) and Nile Red (NR) (5H-Benzo α -phenoxazine-5-one, 9-diethylamino, Sigma-Aldrich, St. Louis, USA) were of analytical

grade.

2.2. Materials

Purified casein micelles were used to monitor our system. They were supplied by Gillot SAS (Saint Hilaire de Briouze, France) and obtained by microfiltration (0.1 μm pore size membrane) of raw skimmed milk followed by diafiltration against milli-Q water and spray dried according to Pierre, Fauquant, Le Graet, and Maubois (1992) and Schuck et al. (1994) on Bionov facilities (Rennes, France). The powder comprised 96% (w/w) proteins – especially caseins (97%) (w/w). Residual whey proteins (3%) (w/w), lactose and diffusible calcium were present in the powder.

Anhydrous milkfat (AMF, melting point 32 °C) was supplied by Corman (Limbourg, Belgium).

2.3. Preparation of different CA suspensions

Casein micelle powder was suspended in milli-Q water at a concentration of 28 g kg^{-1} and NaN_3 (1.6 g kg^{-1}) was added for conservation (Fig. 1A). To ensure good resuspension of the powder, the suspension was stirred at 900 rpm for 6 h at 40 °C in a water bath and then for 16 h at room temperature. The rehydration of the casein micelle powder was checked by laser light diffraction as defined by Schuck, Dolivet, and Jeantet (2012). The results expressed in volume showed that more than 90% of the particles were of size of casein micelles (150 nm diameter). This suspension was used to prepare four CA suspensions (S1, S2, S3 and S4). In S2, S3 and S4 varying amounts of a stock solution of TSC (0.85 mol kg^{-1} in milli-Q water, pH 7.0) were added to reach final concentrations of 4, 13 and 34 mmol kg^{-1} , respectively. S1 was kept as a control

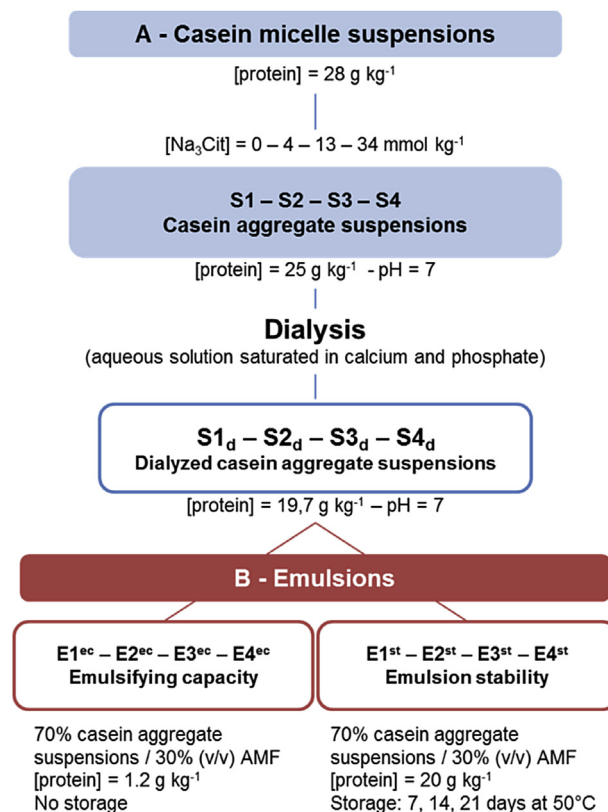


Fig. 1. Preparation of CA suspensions and emulsions. d, ec and st represent « dialyzed », « emulsifying capacity » and « stability », respectively.

suspension (without addition of TSC). These suspensions were stirred for 30 min and then diluted with milli-Q water to reach an intermediate casein concentration of 25 g kg^{-1} . The pH was then adjusted to 7.0 with HCl 1M. S1, S2, S3 and S4 were left overnight at room temperature and the pH of each was readjusted if necessary.

S1, S2, S3 and S4 were then dialyzed against an aqueous solution saturated in calcium and phosphate ($5 \text{ mmol kg}^{-1} \text{ NaH}_2\text{PO}_4 \cdot 2\text{H}_2\text{O}$ and 5 mmol kg^{-1} of $\text{CaCl}_2 \cdot 2\text{H}_2\text{O}$, pH was adjusted to 7.0 using 1 M NaOH). The aim of the dialysis was to remove the added citrate and the ions solubilized from the casein micelle. This provided an identical ionic environment for all the CAs in the four different suspensions. Using a solution saturated in calcium and phosphate also provided the advantage of limiting any further demineralization that might have been induced by classical dialysis against pure water. This was performed in two steps: first the suspensions were individually dialyzed (in separate baths) for 27.5 h at room temperature against a total volume of 44 times each suspension volume, and the baths were changed four times. The second step was combined dialysis (in the same bath) of the four CA suspensions for 15 h at room temperature against a volume 11 times the total suspension volume. The molecular weight cut-off of the dialysis membrane was between 12 and 14 kDa (Spectra/Por, Rancho Dominguez, Canada). The last dialysis bath was then filtered on a $2.5 \mu\text{m}$ filter paper and used to dilute the suspensions to reach a final casein concentration of $19.7 \pm 0.6 \text{ g kg}^{-1}$. The final pH was 6.98 ± 0.04 . The dialyzed CA suspensions, named S1_d, S2_d, S3_d and S4_d, were prepared in duplicate.

2.4. Recovery of the diffusible phases of the CA suspensions

The diffusible phases of each CA suspension were obtained by ultrafiltration for 30 min at 20°C on Vivaspin 20 concentrators (molecular weight cut-off 10 kg mol^{-1} , Vivascience, Palaiseau, France). They were used for the determination of diffusible cation and anion concentrations in the CA suspensions, as well as for the dilution of the CA suspensions and the emulsions for determination of the zeta potentials and sizes.

2.5. Preparation of the two types of emulsion

Two types of emulsion (E^{ec} for “emulsifying capacity” and E^{st} for “stability”) were prepared with each of the four CA suspensions in order to evaluate the emulsifying and emulsion-stabilizing capacity of the CAs (Fig. 1B).

Emulsions E^{ec} were prepared with the CA suspensions diluted at a protein concentration of 1.2 g kg^{-1} with milli-Q water and then added to the 60°C melted AMF at a 30:70 (v/v) ratio. The mixture was emulsified at 50°C in a water bath using a Polytron PT 3100 (Kinematica AG, Littau, Switzerland) at 29,000 rpm for 5 min. Working at a limited protein concentration (1.20 g/kg compared to our emulsification system) highlighted the differences between the CAs by producing emulsions with different droplet sizes.

E^{st} emulsions were prepared following the same procedure except that the CA suspensions were kept at a protein concentration of about 20 g kg^{-1} . In this case, the choice of an excess protein concentration produced emulsions with similar droplet sizes, necessary for the study of the stabilizing capacity of the CAs. E^{st} emulsions were divided into several samples and stored in transparent, cylindrical, hermetically sealed tubes at 50°C for 3 weeks. The temperature of 50°C was chosen in order to prevent the formation of fat crystals in the emulsion that could affect their physical stability (Lopez, Bourgaux, Lesieur, & Ollivon, 2007). Each week, one sample was analyzed by laser light diffraction, electrophoretic light scattering, multiple light scattering and confocal microscopy to follow the evolution of the emulsion. Two replicate emulsions

were made for each type of emulsion.

2.6. Analysis

2.6.1. Mineral composition and distribution

Total cations (calcium, magnesium, sodium and potassium) and diffusible cations and anions (inorganic phosphate, citrate and chloride) were determined in the CA suspensions and in their diffusible phases, respectively. Total anions were determined in the diffusible phases CA suspensions previously acidified at pH 4.6 with a 10% (v/v) acetic acid solution. Cation concentrations were measured by atomic absorption spectrometry (Varian 220FS spectrometer, Les Ulis, France) as described by Brulé, Maubois, and Fauquant (1974). Anion concentrations were determined by ion chromatography (Dionex ICS 3000, Dionex, Voisin le-Bretonneux, France) as described by Gaucheron, Le Graet, Piot, and Boyaval (1996). Colloidal concentrations were deduced by subtracting diffusible from total ion concentrations. The calcium demineralization rates corresponded to the percentage of solubilized calcium compared to total calcium initially present in the suspensions prior to dialysis.

2.6.2. Protein content

Protein content was determined in the CA suspensions and in their respective ultracentrifuged supernatants to deduce the non-sedimentable casein concentrations. The Kjeldahl method (IDF standard 20-1, 2014) was used to determine the total nitrogen concentration in the samples, and a conversion factor of 6.38 was used to convert nitrogen to protein concentration. Measurements were performed in duplicate.

2.6.3. Pellet hydration and sedimentable protein concentrations

Twenty grams of CA suspension were ultracentrifuged at 20°C for 1 h at $100,000 \text{ g}$ (Sorvall Discovery 90 SE, Hitachi, Courtaboeuf, France) and the ultracentrifuged pellets were recovered. Hydration was deduced according to the weight loss after drying the ultracentrifuged pellets of each sample mixed with Fontainebleau sand in an oven at 105°C for 8 h (FIL-IDF Standard 26A, 1993).

Sedimentable protein concentrations were deduced from the proportion of pellets and hydration data by considering that ultracentrifuged pellets consisted mainly of proteins and water (mineral weights were disregarded). Measurements were performed in duplicate.

2.6.4. CA sizes and proportions in the CA suspensions (AsFIFFF)

The molecular weights (MW) and hydrodynamic radii (R_h) of the CAs were determined in suspensions S1_d, S4_d (extreme points), and S2_d (intermediate point) using asymmetrical flow field-flow fractionation (AsFIFFF) coupled to multi angle laser light scattering (MALLS) as described in Guyomarc'h, Violleau, Surel, and Famelart (2010) with slight modifications. A solution saturated in calcium and phosphate (similar to the solution used for the dialysis step) was filtered through $0.1 \mu\text{m}$ filter paper. This filtered solution was used as the eluent for the AsFIFFF separation, and for the ten-fold dilution of the samples.

During the AsFIFFF run, the laminar flow was fixed at 1 mL min^{-1} and only the cross flow varied. The first focusing-injection step (10 min) consisted of setting up the cross flow at 1.5 mL min^{-1} for 1 min. Then $30 \mu\text{L}$ of sample were injected while the cross flow was maintained at 1.5 mL min^{-1} for 9 min. This allowed the analytes to diffuse away from the membrane according to their R_h . The elution step then started with a 5 min plateau at a cross flow rate of 1 mL min^{-1} followed by a linear decrease of 5 min to reach 0.15 mL min^{-1} for 25 min. The cross flow was finally stopped to eliminate all the particles that might have remained in

the AsFIFFF channel.

Under our operating conditions, the AsFIFFF worked in normal mode, which means that larger particles were retained in the channel for longer times than smaller ones, providing that all particles had similar density.

The AsFIFFF was connected to an 18 angle DAWN-DSP MALLS detector (Wyatt Technology, Santa Barbara, CA, USA) ($\lambda = 633$ nm), an Optilab Rex Refractometer (Wyatt Technology, Santa Barbara, CA, USA) ($\lambda = 685$ nm), and an Agilent 1100 UV detector ($\lambda = 280$ nm). The UV signal was used as the source data for measurement of protein concentrations and a calculated extinction coefficient of $9.009 \text{ l g}^{-1} \text{ cm}^{-1}$ was determined and used (bovine serum albumin at 280 nm in the eluent). Astra software version 6.0 was used to analyze the UV and Rayleigh ratio data and determine the MW and R_h values. In this study, it was assumed that the different CAs were spherical and homogenous in composition. R_h were determined between 20 and 28 min (population A) via Berry formalism of a Debye plot.

R_h cannot be calculated directly between 14 and 20 min (populations B and C) because of the low Rayleigh ratio signal in this time range. For suspensions S1_d and S2_d, the R_h values between 20 and 24 min were therefore fitted with a first order exponential model that was extrapolated between 14 and 20 min (populations B and C). This treatment was not possible on S4_d because of the low Rayleigh ratio signal, and the values of R_h determined for S4_d calculated between 20 and 28 min were not accurate enough for their extrapolation (see section 3.1.2).

Similar tests were performed to determine MW values, with slight modifications. The MW values of S1_d and S2_d were fitted with exponential models of first order between 18 and 20 min and the models were extrapolated between 14 and 18 min. In contrast to R_h , the S4_d Rayleigh ratio was high enough to determine MW. For this suspension, the MW values were fitted between 15.5 and 16.5 min (population B) and the model was extrapolated between 14 and 15.5 min (population C).

2.6.5. Zeta potential (ξ)

The electrophoretic mobility of CAs (in CA suspensions) and milkfat droplets (in emulsions) were measured by electrophoretic light scattering using a Zetasizer 3000 HS (Malvern Instruments, Worcestershire, UK). CA suspensions and emulsions were diluted in their corresponding diffusible phases. Diluted CA suspensions were filtered through a $0.45 \mu\text{m}$ pore size membrane to eliminate possible dust particles prior to analysis.

Henry's equation:

$$\zeta = (3\eta\mu/2\epsilon f(Ka)) \quad (1)$$

where η is the viscosity and ϵ the dielectric constant of the solution, was applied to determine the apparent zeta potential (ξ) of the particles from their electrophoretic mobility μ . $F(Ka) = 1.5$ was used according to the Smoluchowski approximation. The measurements for the CA suspensions were performed at 20°C and the viscosity and the dielectric constant of the dissociating medium (water) were 1.00 cp and 80.4, respectively. Measurements for the emulsions were performed at 50°C with a viscosity of 0.55 cp and a dielectric constant of 70.2. Measurements were performed in triplicate.

2.6.6. *vi*. Droplet size distribution in emulsions

The milkfat droplet size distributions were determined by laser light diffraction immediately after the preparation of the emulsions and after 7, 14 and 21 days of storage at 50°C , using a Mastersizer 2000 (Malvern Instruments, Worcestershire, UK) equipped with a He/Ne laser ($\lambda = 633$ nm) and an electroluminescent diode

($\lambda = 466$ nm). The refractive indices were set at 1.46 (at 466 nm) and 1.458 (at 633 nm) for milkfat and 1.33 for water. Before measurements, samples were dispersed in milli-Q water as was, or were previously diluted ten times in a solution of 1% (w/w) SDS to separate aggregated milkfat droplets and estimate the extent of droplet flocculation. All distributions and/or their corresponding mode values (i.e. the maxima of the size distribution) were used to compare the emulsions. Specific surface areas (area per unit mass) were used for the determination of the protein surface concentrations. Measurements were performed in triplicate.

2.6.7. Confocal microscopy of the emulsions

The microscopy observations were carried out with a Nikon Eclipse-TE2000-C1si confocal microscope (Nikon, Champigny sur Marne, France) equipped with argon and He–Ne lasers operating at 488 and 543 nm excitation wavelengths, respectively (emissions were detected between 500 and 530 nm and between 565 and 615 nm, respectively). One milliliter of emulsion was stained using 100 μL of a milkfat soluble Nile Red fluorescent dye solution (0.1% w/w in propane diol) and 50 μL of a Fast green FCF solution (1% w/w in water) to stain the proteins. The samples were left for 15 min at 50°C prior to observation. Microscopy observations were performed at 50°C using a thermal PE100-NI System plate warmer (Linkam Scientific Instruments Ltd., Tadworth Surrey, England). Images were collected with an oil immersion objective with a magnification of $\times 60$. Characteristic images were selected from the 9 images taken for each sample.

2.6.8. Interfacial tension and dilational rheology

An oscillatory drop tensiometer (Tracker, Teclis, France) was used to measure the interfacial tension (γ) and the interfacial dilational moduli (E^* , E' and E'') at the milkfat/CA suspension interfaces, at 50°C . The CA suspensions and the last dialysis bath (control) were used to form a pendant drop of 10 μL at the tip of a syringe that was suspended in an 8 mL cuvette containing melted milkfat (50°C). Two opposite forces, gravity and the force related to γ , were exerted on the drop to induce its shape. Analysis of the shape of the drop 5 min after its formation (equilibrium state) made it possible to calculate the γ value by solving the Laplace equation (Ravera, Loglio, & Kovalchuk, 2010).

Dilational rheology was performed on our system by applying the conditions used by Silva, Saint-Jalmes, de Carvalho, and Gautheron (2014) with slight modifications. Briefly, a sinusoidal oscillation of the drop volume of 10% at a frequency of 0.2 Hz was applied to a 2 min old 10 μL CA suspension drop in the melted milkfat at 50°C . The volume variation engendered a controlled oscillatory compression/dilation of the droplet interfacial area A and resulted in the surface tension oscillation as a function of time $\gamma(t)$. Monitoring of $\gamma(t)$ and determination of its phase shift (ϕ) compared to A(t) made it possible to calculate the complex (E^*), elastic (E') and viscous (E'') moduli of the adsorbed interfacial layer. Purely elastic and solid-like interfacial layers had $E' \gg E''$ and ϕ tended to 0, whereas viscous and fluid-like interfacial layers had $E'' > E'$ and a large ϕ .

2.6.9. Creaming stability ratio

A transparent, cylindrical, hermetically sealed glass tube was filled with 20 mL of fresh Est emulsion and placed in the measurement chamber of a Turbiscan MA2000 multiple light scattering optical analyser Turbiscan MA2000 (Formulation, France). The tube was scanned at 50°C from top to bottom by a 850 nm light source and the back scattered light was recorded every 40 μm . Analysis of the back scattered signal as a function of the height of the tube determined the total height of the emulsion (H) and the thickness of the creamed layer (h). The creaming ratio (r_c) was

defined as $r_c = H/h$. The measurements were performed on each E^{st} emulsion after 0, 7, 14 and 21 days of storage at 50 °C.

2.6.10. Surface protein concentration

The method of separation of the non-adsorbed proteins from the emulsion droplets was derived from Patton and Huston (1986). Forty-four milliliters of E^{st} emulsion were gently mixed with 5 g saccharose in 50 mL centrifuge tubes and maintained at 50 °C in a water bath. The tubes were centrifuged at 200 g for 20 min at 50 °C and frozen at -20 °C. The frozen tubes were cut at the interface to separate the creamed milkfat droplets at the top of the tube and the aqueous phase containing saccharose and non-adsorbed caseins at the bottom. The milkfat droplet phases were transferred to other centrifuged tubes, melted at 50 °C and redispersed in 15 mL of 4% (w/w) SDS solution. The tubes were centrifuged at 1500 g for 20 min at 50 °C, frozen at -20 °C and cut to separate the top milkfat phase from the bottom aqueous SDS phase containing the adsorbed caseins. The first bottom saccharose aqueous phase (containing the non-adsorbed caseins) and the second bottom aqueous SDS phase (containing the adsorbed proteins) were both analyzed in terms of protein concentration using Kjeldahl and micro-Kjeldahl methods, respectively. The amounts of casein adsorbed at the interfaces were related to the specific surface areas of the droplets (previously determined by laser light diffraction) to calculate the interfacial casein concentrations and the percentages of adsorbed caseins.

2.7. Statistics

Measurements were carried out on each of the replicates of suspensions $S1_d$, $S2_d$, $S3_d$ and $S4_d$, emulsions $E1^{ec}$, $E2^{ec}$, $E3^{ec}$ and $E4^{ec}$ and emulsions $E1^{st}$, $E2^{st}$, $E3^{st}$ and $E4^{st}$, except for AsFIFFF, γ and dilatational rheology measurements. The standard deviations were calculated for each determination.

3. Results

The results are presented in two steps with first a focus on the physico-chemical and colloidal characteristics of the CAs in suspensions only. Their functional properties are then described when used as emulsifying agents in our model dairy emulsions.

3.1. Physicochemical characterization of casein aggregate suspensions

3.1.1. Mineral characteristics

Colloidal calcium and inorganic phosphate concentrations (Table 1) decreased simultaneously and in a correlated fashion (Fig. 2) in the order: $S1_d < S2_d < S3_d < S4_d$. This progressive casein micelle demineralization, expressed as a calcium demineralization

Table 1

Distribution of mineral salts in the casein aggregate suspensions. Colloidal concentrations were determined by deducting soluble from total concentrations. The calcium demineralization rates corresponded to the percentage of solubilized calcium compared to total calcium initially present in the suspensions.

	$S1_d$	$S2_d$	$S3_d$	$S4_d$
Diffusible Ca (mmol kg ⁻¹)	0.0	0.0	0.0	0.0
Colloidal Ca (mmol kg ⁻¹)	11.8	10.3	7.5	3.0
Ca demineralization rate (%)	24	35	56	81
Diffusible Pi (mmol kg ⁻¹)	2.1	2.0	1.8	1.8
Colloidal Pi (mmol kg ⁻¹)	3.0	2.5	1.2	0.4
Diffusible Na (mmol kg ⁻¹)	21.5	21.1	21.2	20.6
Colloidal Na (mmol kg ⁻¹)	2.6	2.9	3.6	5.3
Diffusible Cl (mmol kg ⁻¹)	8.3	8.4	8.1	8.0
Colloidal Cl (mmol kg ⁻¹)	0.0	0.0	0.0	0.0

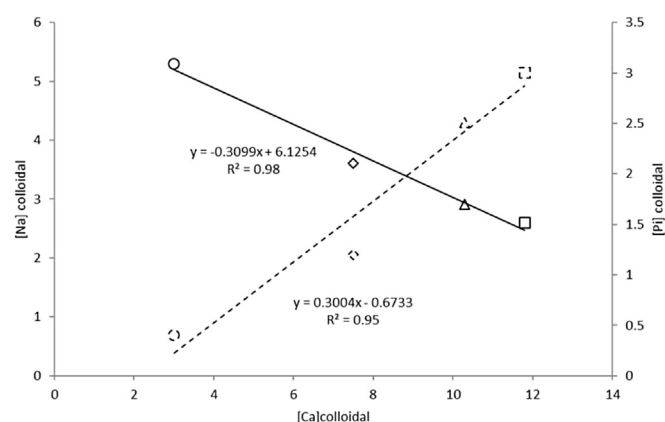


Fig. 2. Correlations between colloidal calcium, sodium and inorganic phosphate concentrations. Colloidal inorganic phosphate (—) and colloidal sodium (---) as a function of calcium for: $S1_d$ (○), $S2_d$ (◇), $S3_d$ (Δ) and $S4_d$ (□).

rate (Table 1), was 24, 35, 56 and 81% for suspensions $S1_d$, $S2_d$, $S3_d$ and $S4_d$, respectively.

On the other hand, the concentration of colloidal sodium (Table 1) increased in the suspensions with the increase in added TSC. This increase was correlated with the decrease in colloidal calcium concentration (Fig. 2), and therefore with the decrease in inorganic phosphate concentration. The chloride ions were only diffusible in the CA suspensions (Table 1). The sodium and chloride present in the saturated dialysis baths (counter ions of phosphate and calcium) mainly contributed to the high colloidal and diffusible concentrations observed in the dialyzed CA suspensions.

Magnesium and potassium were not present in the CA suspensions because these ions were not present in the purified casein micelles. Diffusible ion concentrations (Table 1) were similar in the suspensions and no diffusible or colloidal citrate was found after the dialysis step. Diffusible calcium was close to zero for all suspensions.

3.1.2. Colloid characterization

Hydration of the ultracentrifugation pellets was constant for $S1_d$, $S2_d$ and $S3_d$ and slightly lower for $S4_d$ (Table 2). The concentration of sedimentable proteins decreased with the increase in the amount of TSC added and a reduction of 82% was found when comparing suspension $S1_d$ with $S4_d$ (Table 2). The non-sedimentable casein content thus increased from 8 to 18 g kg⁻¹ with the addition of TSC to the CA suspensions (Table 2).

Similar zeta potentials (22.7 ± 1.3 mV) were measured for each CA suspension (Table 2).

The UV, Rayleigh ratio and the calculated MW and R_h of the CAs in the suspensions obtained by AsFIFFF are represented as a function of elution time, respectively (Fig. 3). For each suspension, three peaks that corresponded to three different populations of particles (A, B and C) were observed by UV:

Population A (19–27 min) corresponded to particles with MW from 7.5×10^7 to 2.5×10^9 g mol⁻¹ in $S1_d$, $S2_d$ and R_h from 30 to 100 nm. Population A in $S4_d$ had MW ranging from 2.2×10^7 to 3.7×10^9 g mol⁻¹, and R_h between 130 and 250 nm. Differences between population A in $S4_d$ and in the other samples must be interpreted with caution because the Rayleigh ratio for this population in $S4_d$ was weak and the MW and R_h values deduced from this signal might be less accurate. Moreover, according to the UV and Rayleigh ratio signals, the largest particles of $S4_d$ suspensions were eluted simultaneously with the largest particles of other suspensions, i.e. $S1$ and $S2_d$ (peaks are superimposed), and therefore these particles had similar MW and R_h .

Table 2
Physicochemical properties of the different CA suspensions.

	S1 _d	S2 _d	S3 _d	S4 _d
Hydration (g of water g ⁻¹ of dried pellet)	3.0 ± 0.1	2.8 ± 0.1	2.6 ± 0.1	2.1 ± 0.1
Non-sedimentable casein (g kg ⁻¹)	8.0 ± 0.5	10.3 ± 0.5	15.0 ± 0.4	18.0 ± 0.8
Sedimentable protein (g kg ⁻¹)	12.9 ± 0.1	11.6 ± 0.1	8.3 ± 1.7	2.3 ± 0.3
Zeta potential of casein aggregates (mV)	-23.5 ± 1.2	-24.4 ± 2.0	-21.5 ± 3.7	-21.5 ± 2.4

Population B particles (15.5–17 min) had R_h between 21 and 26 nm (evaluated on S1_d and S2_d only). Corresponding MW were between 1.4×10^7 and 3.15×10^7 for S1_d and S2_d and between 3.4×10^6 and 1×10^7 for S4_d. Finally, population C (14–15 min) had R_h between 18 and 22 nm (evaluated on S1_d and S2_d only) and MW between 7.0×10^6 and 1.5×10^7 g mol⁻¹ for S1_d and S2_d and between 1.4×10^6 and 3.4×10^6 for S4_d. As for population A, differences between MW in S4_d and in the other samples must be interpreted with caution. Again, UV signals indicated that for all suspensions, the B and C populations of particles eluted simultaneously in S1_d, S2_d, and S4_d. According to the quality of the Rayleigh ratios signals of the suspensions, different data treatments were applied which could explain the differences in the MW values observed.

The proportions of the different populations of particles depended on the amount of added TSC: the largest particles (A) disappeared when the TSC concentration increased, permitting the appearance of the two smallest populations (B and C). Nevertheless, the loss in surface area under the A peak was not equal to the gain in surface area under the B and C peaks due to the fact that the largest particles not only absorbed but also diffused the UV signal compared to small particles that only absorbed the UV signal.

3.2. Functional characterization of casein aggregate suspensions

3.2.1. Emulsifying capacity of casein aggregate suspensions

The particle size distribution profiles of E1^{ec}, E2^{ec}, E3^{ec} and E4^{ec} emulsions are presented in Fig. 4. Given that the size distribution profiles were monomodal, the mode values (*i.e.* the maximum of

each peak) are represented as a function of the added TSC concentration in the CA suspensions (Fig. 4C empty symbols). The distributions shifted to smaller sizes (Fig. 4A, C) as the added TSC concentration increased in the CA suspensions and the mode values varied between 27 and 14 μm. This size range corresponded to macro emulsions. In the presence of SDS, the size distributions of the particles were smaller and narrower than in the absence of SDS (Fig. 4), revealing aggregation of the emulsion droplets. The mean diameter of the emulsion droplets decreased as a function of the increase in TSC concentration in the CA suspension (Fig. 4). Fig. 5 shows confocal micrographs of the fresh E1^{ec}, E2^{ec}, E3^{ec} and E4^{ec} emulsions. Milkfat droplets (in red) were surrounded by casein aggregates (in green). Microstructural observations confirmed the decrease in the size of the emulsion droplets as a function of the increase in TSC concentration in the CA suspensions. Moreover, flocculation of the emulsion droplets was characterized in each emulsion, in agreement with particle size measurements (Fig. 4).

The interfacial tension (γ) at the melted milk fat/CA suspension interface was measured to evaluate the activity of the CAs at the milkfat droplet surface. Blank interfacial tension determined on the last dialysis bath of the CA suspensions was 10 mN m⁻¹. The presence of CAs decreased γ to around 5–6 mN m⁻¹ whatever the added TSC concentration.

3.2.2. Emulsion-stabilizing capacity of the casein aggregate suspensions

The evolution of the creaming ratios (r_c) of Est emulsions over time are shown in Fig. 6. None of the emulsions were stable against

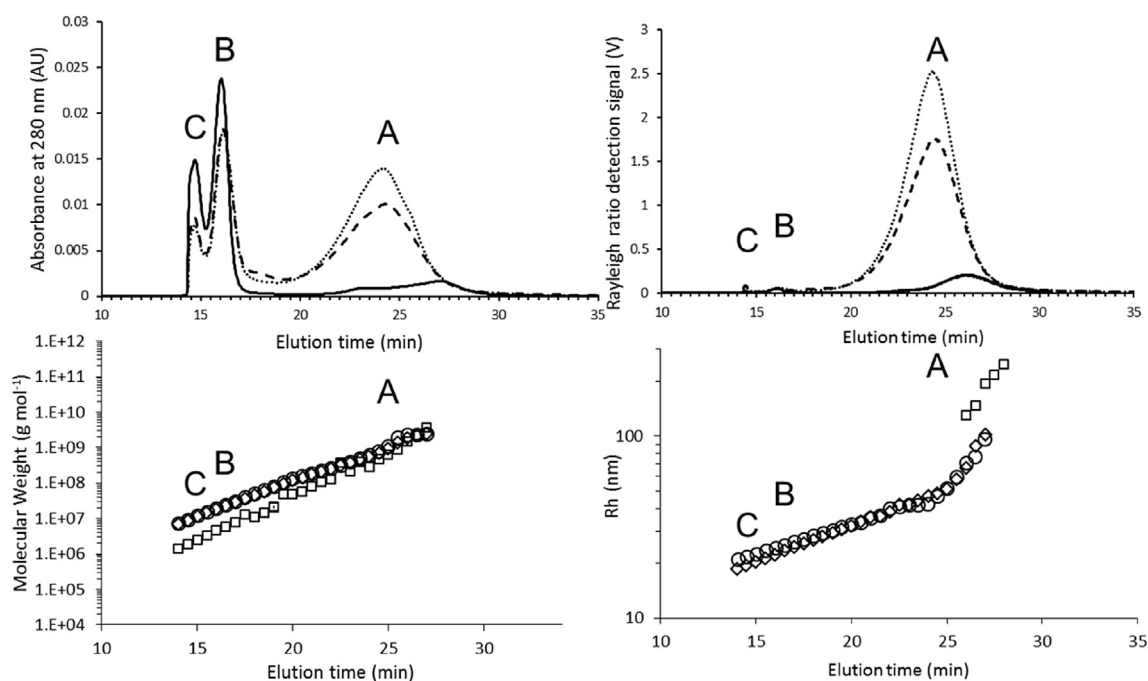


Fig. 3. AsFIFFF determination of structural characteristics of casein aggregates in suspensions. The UV signal (top left), Rayleigh ratio (top right), molecular mass (bottom left) and hydrodynamic radius (bottom right), were determined for the two extreme suspensions S1_d (○)(---), S4_d (□)(—) and one intermediate S2_d (◇)(- - -) CA suspension as a function of the elution time. Casein micelle-like aggregates (population A), sodium caseinate-like aggregates (population B) and protein monomers (population C) are labeled.

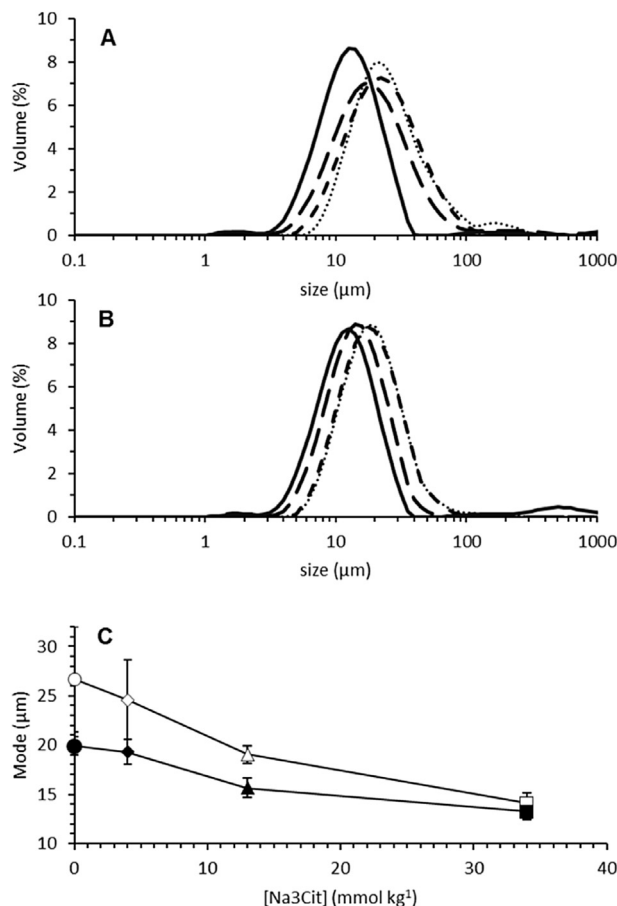


Fig. 4. Size distribution profile of emulsions prepared for the determination of emulsifying capacity (E^{ec}). Emulsions E1^{ec} (○)(·····), E2^{ec} (◇)(---), E3^{ec} (Δ)(—) and E4^{ec} (□)(—) were analyzed as is (A) and diluted ten times in a dissociating medium (aqueous solution of 1% w/w SDS) (B). Evolution of the mode as a function of the concentration of added TSC are represented (C) either in the absence (empty symbols) or presence (filled symbols) of SDS.

creaming. Phase separation was easily observable after 7 days of storage and did not vary during the following 14 days. The determination of r_c indicated that the thickness of the creamed layers decreased with the increase in added TSC in the CA suspensions.

Laser light scattering measurements and confocal microscopy observations were performed on each emulsion throughout storage at 50 °C (Fig. 7). Given that the particle size distribution profiles were monomodal (data not shown), the evolution of the mode value of each emulsion as a function of time is represented. The light scattering measurements were carried out in the presence and absence of SDS. Indeed, this small surfactant is able to dissociate flocculated droplets by replacing the protein at interfaces, permitting discrimination of flocculated droplets from coalesced droplets. When droplets flocculated, the emulsion size distribution shifted to smaller sizes (smaller mode value). In contrast, the addition of SDS had no influence on the size distribution of coalesced droplets. Fig. 7 shows that the size of the particles in emulsions increased with time without SDS, especially for emulsions from CA suspensions containing TSC. For example, the mode value of E2st increased from 12 to 33 μm after 21 days of storage and from 12 to 90 μm for E4st. In the presence of SDS, the size distribution of the droplets did not evolve over time, the mode being 12 μm, similar to the size determined after the preparation of the emulsions (data not shown). These constant values indicated that E2st, E3st and E4st were destabilized by flocculation but were stable against

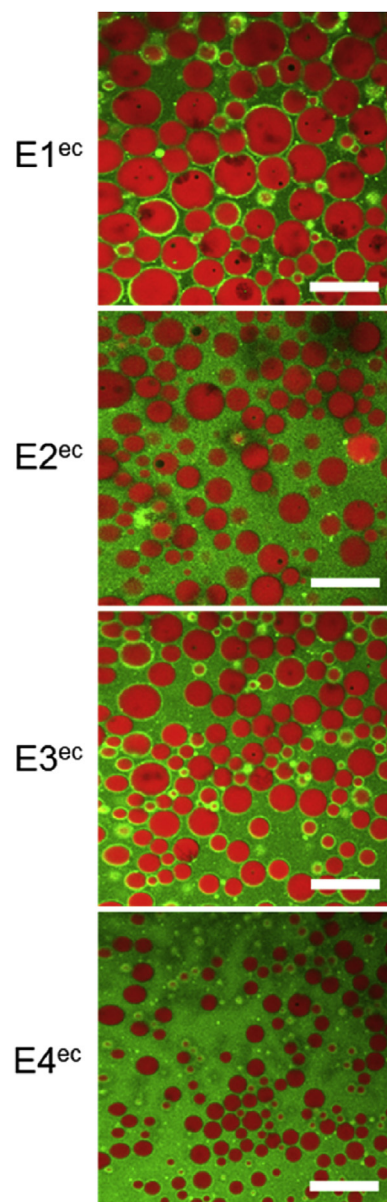


Fig. 5. Confocal laser scanning microscopy images of the emulsions prepared for determination of emulsifying capacity (E^{ec}). Microscopic images were recorded at 50 °C using a thermal plate warmer. Milkfat emulsion droplets (in red) surrounded by casein (in green). Scale bars measure 50 μm. (For interpretation of the references to colour in this figure legend, the reader is referred to the web version of this article.)

coalescence. The E1st emulsion, which maintained a constant mode value throughout storage, was stable against both flocculation and coalescence phenomena.

The corresponding micrographs of each emulsion at each time-point were in good agreement with laser light scattering data (Fig. 7). Each emulsion maintained the same droplet size during storage. However, some micrographs showed contrast differences, with bright milkfat droplets at the foreground of the image and dark red droplets at the back. This color variation was attributed to the appearance of 3D milkfat droplet flocs in the emulsions that coexisted on different focal planes of the micrographs. According to the microscopy observations, E3st and E4st emulsions were the most highly flocculated under our storage conditions.

The zeta potential of individual emulsion droplets and flocculated droplets did not evolve significantly during the 21 days of

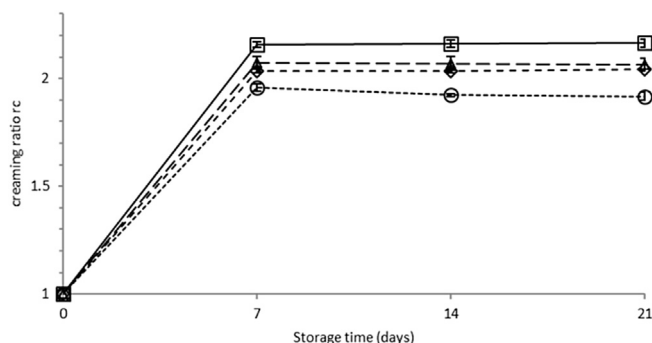


Fig. 6. Time evolution of creaming ratios r_c of emulsions prepared for the determination of emulsion stability (E^{st}). Creaming ratio defined as $r_c = H/h$ where H is the total height of the emulsion and h the thickness of the creamed layer. Standard deviation bars are represented behind the point marks.

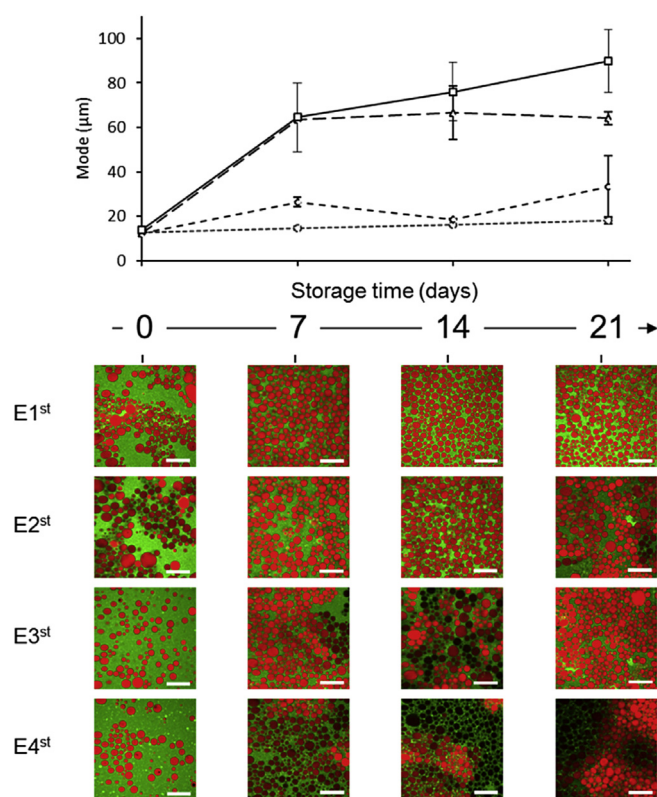


Fig. 7. Microscopic evolution of the emulsions over time (E^{st}). Droplet size (mode) and confocal micrograph evolution as a function of storage time: $E1^{st}$ (○)(---), $E2^{st}$ (◇)(- - -), $E3^{st}$ (Δ)(—) and $E4^{st}$ (□)(____). Microscopy images were recorded at 50 °C using a thermal plate warmer. Milkfat emulsion droplets (in red) are surrounded by casein (in green). Contrast differences are attributed to the appearance of 3D milkfat droplet flocs in the emulsion that coexisted on different focal planes of the micrographs. (For interpretation of the references to colour in this figure legend, the reader is referred to the web version of this article.)

storage (23.1 ± 1.4 mV).

Around $24 \pm 1\%$ of the total protein present in the emulsions was adsorbed at the interface, whatever the type of CA suspension used to make the emulsion, which corresponded to a casein surface concentration of around 17.4 ± 0.7 mg m^{-2} .

The interfacial dilatational moduli (E^* , E' and E'') were determined at the melted milkfat/CA suspensions interface. All suspensions presented similar values: 14.6 ± 0.4 , 14.4 ± 0.4 and 2.9 ± 0.2 for complex (E^*), elastic (E') and viscous (E'') moduli, respectively.

The contribution of E' to E^* was higher than the E'' contribution, reflecting solid-like behavior of the adsorbed casein aggregate layers.

4. Discussion

The results are discussed in two stages, with first a focus on the characterization of the CA suspensions in terms of mineralization and colloidal properties. The second stage consisted of investigation of the emulsifying and emulsion-stabilizing capacity of the CA used as emulsifying agents in two types of model dairy emulsions.

4.1. Characterization of the different CA suspensions

4.1.1. Addition of TSC resulted in progressive casein micelle demineralization

Analysis of the distribution of minerals confirmed that TSC had an influence on the mineralization of the casein micelle. By chelating the diffusible calcium, citrate ions induced the progressive removal of the colloidal calcium (Gaucheron, 2004). This was in accordance with results reported by many authors who recorded citrate chelation of calcium either by determining calcium activity (Johnston & Murphy, 1992; Udabage, McKinnon, & Augustin, 2001; de Kort et al., 2011), or diffusible calcium and/or colloidal calcium concentrations (Le Ray et al., 1998; Mizuno & Lucey, 2005; Mohammad & Fox, 1983; Odagiri & Nickerson, 1965; Ozcan-Yilsay, Lee, Horne, & Lucey, 2007; Vujicic, deMan, & Woodrow, 1968) in milk or micellar suspensions.

The simultaneous and correlated decrease in the colloidal inorganic phosphate concentration (Fig. 2) was attributed to the solubilization of the colloidal calcium phosphate (Le Ray et al., 1998; Mizuno & Lucey, 2005; Mohammad & Fox, 1983). Increasing the concentration of TSC therefore led to progressive calcium phosphate demineralization of the CA suspensions.

Furthermore, the correlation observed between the colloidal concentrations of calcium and sodium (Fig. 2) suggested that the negative charges induced by the calcium demineralization (presence of free phosphoserine residues) were screened by monovalent sodium ions, potentially explaining the constant zeta potential observed for each CA suspension (Table 2).

Mineral content was also modified by the casein powder resuspension and dialysis steps. Determination of colloidal and diffusible calcium in S1 (prior to dialysis – data not shown) and S1_d (after dialysis) induced partial solubilization of the colloidal calcium. This limited calcium demineralization (24%, reported in Table 1) was attributed to the resuspension of the purified casein micelle powder in water and to the dialysis step.

The dialysis step also permitted removal of the added citrate and established a similar diffusible phase in the four suspensions (Table 1). As the result, the ionic strengths of all the suspensions were taken to be similar in the four suspensions.

4.1.2. TSC demineralization resulted in disaggregation of the casein micelle

Structural modifications of the CA were observed parallel to the micellar demineralization. The quantity of sedimentable proteins was reduced and that of non-sedimentable proteins consistently increased (Table 2), which showed progressive dissociation of the CAs. Similar trends were reported by Udabage et al. (2001), Le Ray et al. (1998) and de Kort et al. (2011).

AsFIFFF characterization was performed in order to evaluate the sizes of the dissociated CAs. This revealed that three populations of particles of different sizes and proportions were simultaneously present in the CA suspensions (Fig. 3). Population A consisted of large CA with MW and R_h comparable to those of the casein micelle

(MW between 5×10^7 and 1×10^{10} g mol⁻¹ and r_{rms} of 50–350 nm), as previously reported (Glantz, Håkansson, Lindmark Månsson, Paulsson, & Nilsson, 2010; Pitkowski et al., 2008). The addition of TSC induced dissociation of these aggregates and increased the proportion of population B. This population consisted of aggregates similar to sodium caseinate particles with MW of $4-9 \times 10^6$ g mol⁻¹ and R_h between 10–20 nm, as reported by Lucey, Srinivasan, Singh, and Munro (2000). Using 50 times more TSC per gram of protein than in our study, Panouillé, Nicolai, and Durand (2004) reported slightly smaller CAs (MW = 2×10^5 g mol⁻¹ and R_h = 12 nm). Finally, population C corresponded to the smallest particles in our suspensions. The percentage of these small particles was also increased by the increased addition of TSC. This suggested that population C corresponded to casein monomers dissociated from the larger CAs. According to Guyomarc'h et al. (2010) and Glantz et al. (2010), they could also be attributed to residual whey protein monomers.

As demonstrated by Pitkowski, Nicolai, and Durand (2007), Lin, Leong, Dewan, Bloomfield, and Morr (1972) and Marchin et al. (2007) with polyphosphate and EDTA calcium chelation, the dissociation of casein micelles by calcium chelating agents is a “cooperative process” in which the structure of the casein micelle remains intact (large aggregates) or becomes fully dissociated (small aggregates of the same size are produced). In other words, the dissociation of the casein micelle does not provide aggregates of intermediate sizes. The three populations of particles (casein micelle-like aggregates, sodium caseinate-like aggregates, and protein monomers) and their dependence on the amount of TSC added confirmed that the “cooperative process” can be applied to the TSC dissociation of casein micelles.

The hydration measurements of S1_d, S2_d, S3_d and S4_d pellets (Table 2) differed from the findings of Le Ray et al. (1998) who reported that the water content of the sedimented CAs increased with the addition of TSC. This was also supported by the voluminosity data determined by de Kort et al. (2011). Compared to our study, these authors did not monitor the diffusible phases of their suspensions. The dialysis step and thus the diffusible environment of the sedimentable casein aggregates therefore seemed to have an

impact on their hydration.

As expected, TSC demineralized and dissociated the casein micelle to different extents in order to produce four suspensions containing various CAs. The effects of a calcium chelating agent on the casein micelle seemed to be in good agreement with the use of an ion-exchange resin to sequester the calcium ((Xu et al., 2016; Ye, 2011). Xu et al. (2016) reported a similar dissociation of the casein micelle into smaller CAs and a decrease in the total calcium content of their casein micelle suspension. These authors also reported that, beyond a level of 20% of calcium demineralization (which is lower than the demineralization rate of our four suspensions), the dissociated caseins present in the ultracentrifuged supernatant (non-sedimentable proteins) were of similar composition to that of the native casein micelle. This suggests that the micelle-like CAs and the mixture of sodium-caseinate CAs and the “free” casein monomers have the same composition.

This first step of our study was necessary to characterize and control our CA suspensions accurately in order to elucidate their emulsifying and emulsion-stabilizing capacity. To summarise, suspension S1_d mostly contained highly mineralized and large casein micelle-like CAs. Intermediate suspensions (S2_d and S3_d) contained a mixture of both large and small sodium caseinate-like CAs, with a small quantity of “free” casein monomers. Finally, S4_d mainly consisted of poorly mineralized small CAs, “free” casein monomers and residual traces of large CAs (Fig. 8A).

4.2. Investigation of CA capacity as emulsifying agents

4.2.1. Decreasing the size of the CA increased its emulsifying capacity

The emulsifying capacity of a protein (or a protein aggregate) can be characterized by measuring the emulsion droplet size at a particular protein concentration: the smaller the droplet, the better the protein aggregate as an emulsifier (Euston & Hirst, 1999). Differences in emulsifying capacity can generally be attributed to the surface activity and/or to the size of the emulsifying agent: the higher the surface activity and/or the smaller the size, the greater the emulsifying capacity.

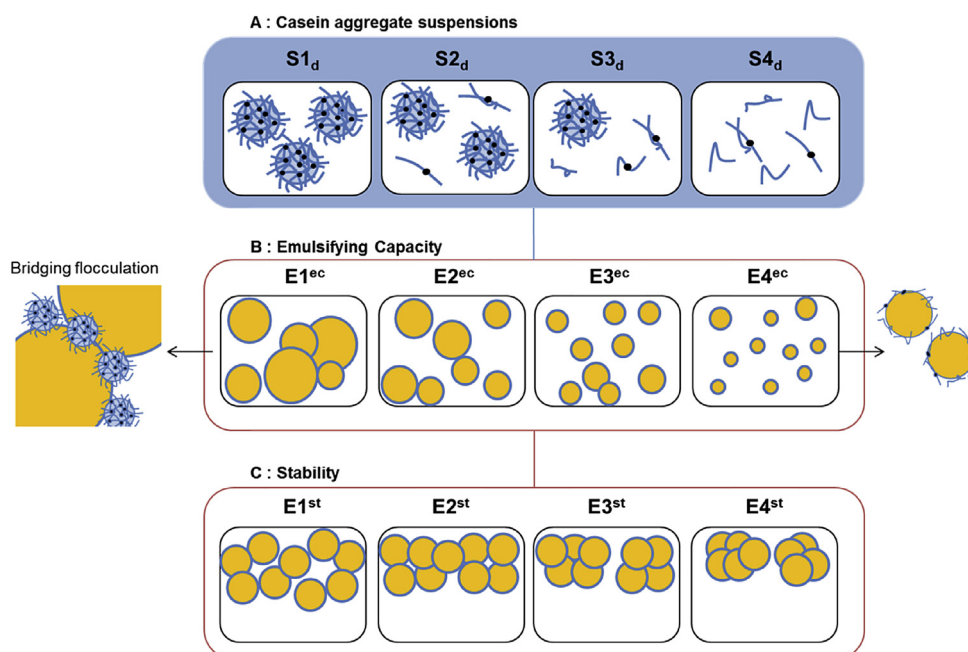


Fig. 8. Diagrams of the CA suspensions (A), the emulsions prepared for determination of the emulsifying capacity (B) and the stabilizing capacity (C) of the casein aggregates.

Emulsion size distribution profiles and micrographs (Figs. 4 and 5) clearly indicated differences in emulsifying capacity which depended on the CA suspension used. The presence of small CAs facilitated the blending of the milkfat, making it possible to form emulsions with a smaller droplet size, and protected the emulsions against the appearance of bridging flocculation between the milkfat droplets (Fig. 8B).

The surface tension, γ , is characteristic of the surface activity of the CA, i.e. how effective CAs are at reducing unfavorable interactions between the milkfat and the suspension (McClements, 2005). For the concentrations used here, the surface tension measurements at the milk fat/CA suspension interfaces revealed that large micelle-like and small sodium caseinate-like CAs had the same ability to reduce the unfavorable interactions between the two phases ($5\text{--}6\text{ mN m}^{-1}$). All the samples had the same surface tension at equilibrium (obtained after 5 min) and hence the same surface coverage.

Our results, showing that there was no difference in equilibrium between our samples, differed from those of Courthaudon et al. (1999), who found that sodium caseinate was more surface active than casein micelles. However, this strongly depends on the concentrations studied: in the study reported here we used a fairly high concentration (20 g/kg) and the interfacial layer was obtained at equilibrium by the combined adsorption of the free casein monomers, the sodium caseinate-like CAs and the micelle-like CAs, which ruptured once adsorbed. Indeed, measurements at a concentration of 1.2 g/kg also provided the same surface tensions and rheological properties (whatever the state of aggregation – data not shown), meaning that at a concentration of 20 g/kg there was a large reservoir of proteins in the bulk, compared to the quantity that could be adsorbed.

It is not possible from these measurements to simply ascribe the differences in emulsifying properties to different surface activities of the types of aggregates. Nevertheless, as we also report here, Courthaudon et al. (1999), Ye (2011), Mulvihill and Murphy (1991) and Euston and Hirst (1999) established a correlation between the state of aggregation of the caseins and their emulsifying capacity.

For further analysis, it is important to note that we were not able to monitor the dynamics of adsorption at short timescales t (typically for $t < 2\text{ s}$). However, our results showed that the surface tension had already decreased significantly during this short non-monitored period. There might therefore have been differences in the dynamics of adsorption between the samples at very short timescales (those having the highest concentrations of monomers reducing the surface tension more rapidly).

In fact, the emulsion production process was rapid, and the associated timescale was also in the order of 1 s. Understanding the differences between emulsifying properties may therefore require monitoring of the surface coverage at such short timescales (less than 1 s). Many small, mobile casein units, such as casein monomers and sodium caseinate-like CAs are thus available for rapid adsorption and to emulsify greater amounts of milkfat/suspension interface at high concentrations of TSC. In contrast, when not enough casein units were present in the suspension to adsorb on the generated interface rapidly (e.g. E1^{ec}), the milkfat droplets coalesced until all their surfaces were covered, thus making the emulsions coarser. Large micelle-like CAs also had the ability to share between two independent droplets and induce bridging flocculation (Fig. 8B).

4.2.2. Emulsions were stable against coalescence but creamed and flocculated

Destabilization of emulsions can result from three phenomena i.e. creaming, flocculation and coalescence. The Est emulsions were designed to have identical droplet sizes, despite the differences in

CA suspension emulsifying capacity used to prepare them. This approach removed the influence of the droplet size on the creaming, flocculation and coalescence phenomena.

Visual observations (Fig. 6) and emulsion size measurements (Fig. 7) as a function of time showed that the emulsions remained stable against coalescence throughout storage. However, emulsions were destabilized by creaming and flocculation (Fig. 7).

4.2.3. The adsorbed CAs contributed to coalescence stability whatever their state of aggregation

The stability of the emulsions against coalescence is generally correlated with the characteristics of the CA layers adsorbed at the droplet surface. Interfacial casein concentrations and surface tension values provided information on the extent of casein adsorption at the interface, and dilational rheology determined how strongly proteins were adsorbed and interacted at the interface (McClements, 2005).

As with the surface tension data, the surface casein concentrations were also similar (17.4 mg m^{-2}) and independent of the type of CA used to form each emulsion. Our values were between those found by Euston and Hirst (1999) on milk casein concentrate (21 mg m^{-2}) and Courthaudon et al. (1999) on casein micelles (10 mg m^{-2}). Our values were 6–8 times higher than the values reported for sodium caseinate (2.3 mg m^{-2} by Euston and Hirst (1999), 3 mg m^{-2} by Dickinson, Golding, and Povey (1997), 1 mg m^{-2} by Dickinson and Golding (1997) and 1.63 mg m^{-2} by Courthaudon et al. (1999)). Our measurements thus fall within the highest reported values for interfacial concentration, and can be interpreted as a thick layer of adsorbed proteins, in agreement with the fact that we were using high protein concentrations, such that the interfacial properties did not depend on the concentration and that we had a large excess of proteins in bulk.

Dilational rheology measurements demonstrated that adsorbed layers of CAs had similar solid-like behaviors ($E' \gg E''$) whatever the state of aggregation of the casein used to form the emulsion. Large CAs spread out at the interface, and intermolecular interactions within the adsorbed layers were similar. The wide contribution of E' to E^* ($E \gg E''$) was in agreement with the literature on sodium caseinate at diverse oil/water interfaces (Amine, Dreher, Helgason, & Tadros, 2014; Benjamins, Cagna, & Lucassen-Reynders, 1996). These two results suggested that the state of aggregation of the casein was not decisive for the stability of the emulsions against coalescence.

4.2.4. Creaming and flocculation enhanced each other

Creaming is due to the difference in density between the milkfat and the aqueous suspension phases of the emulsions. This phenomenon was enhanced by the large size of the individual milkfat droplets ($12\text{ }\mu\text{m}$). In our case, creaming (Fig. 6) and flocculation (Fig. 7) only occurred during the first week of storage, suggesting that these two concomitant phenomena influenced each other. On the one hand, creaming was intensified by the formation of milkfat droplet combination due to flocculation. On the other hand, flocculation was favored by the creaming that moved the droplets forward and encouraged their contact, which is a necessary step for the final destabilization of flocculation to occur (Dauphas, Amestoy, Llamas, Anton, & Riaublanc, 2008). However, the nature of the CA and the environment also had a role in the appearance of flocculation.

4.2.5. Unabsorbed CAs induced depletion-flocculation of the emulsion droplets

Depletion-flocculation is an instability mechanism that occurs in emulsions and is induced by the presence of unabsorbed particles. It takes place when two neighboring droplets are close enough

to exclude any unabsorbed particles from the gap that separates them. Consequently, an osmotic pressure gradient is induced that causes net attraction between the emulsion droplets (Asakura & Oosawa, 1958; Dickinson & Golding, 1997, 1998; Dickinson et al., 1997; Radford & Dickinson, 2004). This phenomenon was observed in our emulsions because of the presence of unabsorbed CAs.

The evolution of the milkfat droplet sizes in the emulsion as a function of time (Fig. 7) revealed that increases in percentage of small CAs in the emulsions augmented flocculation of the milkfat droplets. This was in agreement with the results obtained on native casein micelles, calcium-depleted casein micelles, calcium caseinate and sodium caseinate (Dickinson & Golding, 1998; Euston & Hirst, 1999; Srinivasan, Singh, & Munro, 2001; Ye, 2011). These reported studies demonstrated that the depletion-flocculation process was strongly dependent on the state of aggregation of the casein. Furthermore, small CAs were of the optimum size (20 nm) to cause the greatest depletion-flocculation of emulsion droplets (Radford & Dickinson, 2004).

4.2.6. CA environment (mineral equilibrium and storage temperature) influenced the sticking of the emulsion droplets

Finally, storage temperatures higher than 37 °C can induce gelation by flocculation of sodium caseinate and β casein emulsions if a sufficient amount of added calcium is present in the emulsion aqueous phase (Dauphas et al., 2008; Dickinson & Casanova, 1999; Dickinson & Eliot, 2003; Eliot & Dickinson, 2003). Added calcium reduces the steric repulsion between the emulsion droplets by binding to the adsorbed caseins, and high temperature encourages hydrophobic interactions between caseins and promotes sticking behavior (Dauphas et al., 2008; Dickinson & Casanova, 1999). However, no calcium was present in the diffusible phases of the emulsions as it was not present in the CA suspensions (Table 1). Moreover, the extent of flocculation increased when the colloidal calcium content of the CAs decreased. This suggested that sodium ions reduced steric repulsion between the emulsion droplets in our system. This hypothesis was supported by the increased colloidal sodium content in the CA suspensions (Table 1) and the constant zeta potential values (23.1 ± 1.4 mV) measured on Est emulsions throughout storage. Because of their highly aggregated state, large and strongly mineralized CAs were also less inclined to link with their counterparts adsorbed on separated milkfat droplets or suspended in the bulk emulsion phases.

5. Conclusion

Varying the concentration of added TSC in pure casein micelle suspensions produced four CA suspensions that were progressively demineralized and dissociated. The diffusible phases of these suspensions were monitored with a dialysis step. The use of these CAs as emulsifying agents in our model dairy emulsions revealed differences in emulsifying and emulsion-stabilizing properties. The smaller CAs had better emulsifying capacity as their presence favored the formation of emulsions with smaller droplet sizes. The surface activity of the four CA suspensions was similar and the differences in emulsifying capacity were attributed only to variation of the state of aggregation of the CAs. With regard to the stabilizing capacity of the CAs, all the emulsions were unstable under our storage conditions (21 days, 50 °C). Creaming was promoted by the presence of large droplets in the emulsions and favored the occurrence of flocculated droplets. Flocculation was also enhanced by the presence of small, demineralized CAs. However, all the emulsions remained stable against coalescence during storage. This was probably due to the presence of similar quantities of adsorbed CAs at the surface of the emulsion droplets that formed protective

layers with similar viscoelastic properties. Combining the results obtained on the CAs in suspension with the emulsion properties revealed that the state of aggregation of the CAs had a major impact on their emulsifying capacity and emulsion-stabilizing properties. Modulating the mineral content of the casein micelle is therefore an interesting method for optimization of emulsion functionality. Further studies on CA composition and nanostructure, both in suspension and adsorbed at the milkfat/water interface, would improve understanding of the differences between the emulsifying and emulsion-stabilizing properties. In this case, the destabilization of the emulsions in the early stages should be studied for a better understanding of the involved phenomena. As an extension of this work, investigation of the rheology of the creamed layers of the emulsions is planned as well as the assessment of other functionalities of newly formed CAs.

Acknowledgements

The authors thank the French Dairy Interbranch Organization (CNIEL) for their financial support, Rachel Boutrou for assistance with writing the manuscript and Anne-Laure Chapeau for proof reading the article.

References

- Amine, C., Dreher, J., Helgason, T., & Tadros, T. (2014). Investigation of emulsifying properties and emulsion stability of plant and milk proteins using interfacial tension and interfacial elasticity. *Food Hydrocolloids*, 39, 180–186.
- Asakura, S., & Oosawa, F. (1958). Interaction between particles suspended in solutions of macromolecules. *Journal of Polymer Science*, 33(126), 183–192.
- Barbosa-Cánovas, G. V., Kokini, J. L., Ma, L., & Ibarz, A. (1996). The rheology of semiliquid foods. In *Advances in food and nutrition research* (Vol. 39, pp. 1–69). Elsevier.
- Benjamins, J., Cagna, A., & Lucassen-Reynders, E. H. (1996). Viscoelastic properties of triacylglycerol/water interfaces covered by proteins. *Colloids and Surfaces A: Physicochemical and Engineering Aspects*, 114, 245–254.
- Broyard, C., & Gaucheron, F. (2015). Modifications of structures/functions of caseins: a scientific and technological challenge. *Dairy Science & Technology*, 95, 831–862.
- Brulé, G., Maubois, J.-L., & Fauquant, J. (1974). Etude de la teneur en éléments minéraux des produits obtenus lors de l'ultrafiltration du lait sur membrane. *Lait*, 539–540, 600–615.
- Courthaudon, J.-L., Girardet, J.-M., Campagne, S., Rouhier, L.-M., Campagna, S., Linden, G., et al. (1999). Surface active and emulsifying properties of casein micelles compared to those of sodium caseinate. *International Dairy Journal*, 9(3–6), 411–412.
- Dalgleish, D. G., & Corredig, M. (2012). The structure of the casein micelle of milk and its changes during processing. *Annual Review of Food Science and Technology*, 3(1), 449–467.
- Dauphas, S., Amestoy, M., Llamas, G., Anton, M., & Riaubanc, A. (2008). Modification of the interactions between β -casein stabilized oil droplets with calcium addition and temperature changing. *Food Hydrocolloids*, 22(2), 231–238.
- Dickinson, E. (1999). Caseins in emulsions: Interfacial properties and interactions. *International Dairy Journal*, 9(3–6), 305–312.
- Dickinson, E., & Casanova, H. (1999). A thermoreversible emulsion gel based on sodium caseinate. *Food Hydrocolloids*, 13(4), 285–289.
- Dickinson, E., & Eliot, C. (2003). Defining the conditions for heat-induced gelation of a caseinate-stabilized emulsion. *Colloids and Surfaces B: Biointerfaces*, 29(2–3), 89–97.
- Dickinson, E., & Golding, M. (1997). Depletion flocculation of emulsions containing unabsorbed sodium caseinate. *Food Hydrocolloids*, 11(1), 13–18.
- Dickinson, E., & Golding, M. (1998). Influence of calcium ions on creaming and rheology of emulsions containing sodium caseinate. *Colloids and Surfaces A: Physicochemical and Engineering Aspects*, 144(1–3), 167–177.
- Dickinson, E., Golding, M., & Povey, M. J. W. (1997). Creaming and flocculation of oil-in-water emulsions containing sodium caseinate. *Journal of Colloid and Interface Science*, 185(2), 515–529.
- Eliot, C., & Dickinson, E. (2003). Thermoreversible gelation of caseinate-stabilized emulsions at around body temperature. *International Dairy Journal*, 13(8), 679–684.
- Euston, S. R., & Hirst, R. L. (1999). Comparison of the concentration-dependent emulsifying properties of protein products containing aggregated and non-aggregated milk protein. *International Dairy Journal*, 9(10), 693–701.
- Foegeding, E. A., & Davis, J. P. (2011). Food protein functionality: A comprehensive approach. *Food Hydrocolloids*, 25(8), 1853–1864.
- Gaucheron, F. (2004). *Minéraux et produits laitiers*. Paris: Technique & Documentation.

- Gaucheron, F., Le Graet, Y., Piot, M., & Boyaval, E. (1996). Determination of anions of milk by ion chromatography. *Le Lait*, 76(5), 433–443.
- Glantz, M., Håkansson, A., Lindmark Månsson, H., Paulsson, M., & Nilsson, L. (2010). Revealing the size, conformation, and shape of casein micelles and aggregates with asymmetrical flow field-flow fractionation and multiangle light scattering. *Langmuir*, 26(15), 12585–12591.
- Guyomarc'h, F., Violleau, F., Surel, O., & Famelart, M.-H. (2010). Characterization of heat-induced changes in skim milk using asymmetrical flow field-flow fractionation coupled with multiangle laser light scattering. *Journal of Agricultural and Food Chemistry*, 58(24), 12592–12601.
- Guzey, D., & McClements, D. J. (2006). Formation, stability and properties of multilayer emulsions for application in the food industry. *Advances in Colloid and Interface Science*, 128–130, 227–248.
- Holt, C., Carver, J. A., Ecroyd, H., & Thorn, D. C. (2013). Caseins and the casein micelle: Their biological functions, structures, and behavior in foods. *Journal of Dairy Science*, 96(10), 6127–6146.
- Holt, C., & Horne, D. S. (1996). The hairy casein micelle: Evolution of the concept and its implications for dairy technology. *Nederlands Melk En Zuiveltijdschrift*, 50(2), 85–111.
- International Dairy Federation. (1993). *Lait et crème en poudre - Détermination de la teneur en eau*. International Standard FIL-IDF 26A.
- International Dairy Federation. (2014). *Milk and milk products - Determination of nitrogen content - Part 1: Kjeldahl principle and crude protein calculation*.
- Johnston, D. E., & Murphy, R. J. (1992). Effects of some calcium-chelating agents on the physical properties of acid-set milk gels. *Journal of Dairy Research*, 59(02), 197.
- de Kort, E., Minor, M., Snoeren, T., van Hooijdonk, T., & van der Linden, E. (2011). Effect of calcium chelators on physical changes in casein micelles in concentrated micellar casein solutions. *International Dairy Journal*, 21(12), 907–913.
- Le Ray, C., Maubois, J.-L., Gaucheron, F., Brulé, G., Pronnier, P., & Garnier, F. (1998). Heat stability of reconstituted casein micelle dispersions: Changes induced by salt addition. *Le Lait*, 78(4), 375–390.
- Lin, S. H. C., Leong, S. L., Dewan, R. K., Bloomfield, V. A., & Morr, C. V. (1972). Effect of calcium ion on the structure of native bovine casein micelles. *Biochemistry*, 11(10).
- Lopez, C., Bourgaux, C., Lesieur, P., & Ollivon, M. (2007). Coupling of time-resolved synchrotron X-ray diffraction and DSC to elucidate the crystallization properties and polymorphism of triglycerides in milk fat globules. *Le Lait*, 87(4–5), 459–480.
- Lucey, J. A., Srinivasan, M., Singh, H., & Munro, P. A. (2000). Characterization of commercial and experimental sodium caseinates by multiangle laser light scattering and size-exclusion chromatography. *Journal of Agricultural and Food Chemistry*, 48(5), 1610–1616.
- Marchin, S., Putaux, J.-L., Pignon, F., & Léonil, J. (2007). Effects of the environmental factors on the casein micelle structure studied by cryo transmission electron microscopy and small-angle x-ray scattering/ultras-small-angle x-ray scattering. *The Journal of Chemical Physics*, 126(4), 045101.
- McClements, D. J. (2005). *Food emulsions principles, practices, and techniques*. Boca Raton: CRC Press.
- Mizuno, R., & Lucey, J. A. (2005). Effects of emulsifying salts on the turbidity and calcium-phosphate-protein interactions in casein micelles. *Journal of Dairy Science*, 88(9), 3070–3078.
- Mohammad, K. S., & Fox, P. F. (1983). Influence of some polyvalent organic acids and salts on the colloidal stability of milk. *International Journal of Dairy Technology*, 36(4), 112–117.
- Mulvihill, D. M., & Murphy, P. C. (1991). Surface active and emulsifying properties of caseins/caseinates as influenced by state of aggregation. *International Dairy Journal*, 1(1), 13–37.
- Odagiri, S., & Nickerson, T. A. (1965). Complexing of calcium by hexametaphosphate, oxalate, citrate, and ethylenediamine-tetraacetate in milk. II. Dialysis of milk containing complexing agents. *Journal of Dairy Science*, 48(1), 19–22.
- Ozcan-Yilsay, T., Lee, W.-J., Horne, D., & Lucey, J. A. (2007). Effect of trisodium citrate on rheological and physical properties and microstructure of yogurt. *Journal of Dairy Science*, 90(4), 1644–1652.
- Panouillé, M., Nicolai, T., & Durand, D. (2004). Heat induced aggregation and gelation of casein submicelles. *International Dairy Journal*, 14(4), 297–303.
- Patton, S., & Huston, G. E. (1986). A method for isolation of milk fat globules. *LIPIDS*, 21(2), 170–174.
- Pierre, A., Fauquant, J., Le Graet, Y., & Maubois, J.-L. (1992). Préparation de phosphocaseinate natif par microfiltration sur membrane. *Lait*, 72, 461–474.
- Pitkowski, A., Durand, D., & Nicolai, T. (2008). Structure and dynamical mechanical properties of suspensions of sodium caseinate. *Journal of Colloid and Interface Science*, 326(1), 96–102.
- Pitkowski, A., Nicolai, T., & Durand, D. (2007). Scattering and turbidity study of the dissociation of the casein by calcium chelation. *Biomacromolecules*, 9, 369–375.
- Radford, S. J., & Dickinson, E. (2004). Depletion flocculation of caseinate-stabilized emulsions: What is the optimum size of the non-adsorbed protein nano-particles? *Colloids and Surfaces A: Physicochemical and Engineering Aspects*, 238(1–3), 71–81.
- Ravera, F., Loglio, G., & Kovalchuk, V. I. (2010). Interfacial dilational rheology by oscillating bubble/drop methods. *Current Opinion in Colloid & Interface Science*, 15(4), 217–228.
- Schmidt, D. T., & Payens, T. A. J. (1976). Micellar aspects of casein. In *Surface colloid science volume 9* (Vol. 9, pp. 165–229). New York: John Wiley & Sons. Matijević E.
- Schuck, P., Dolivet, A., & Jeantet, R. (2012). *Analytical methods for food and dairy powders*. Chichester, West Sussex; Ames, Iowa: Wiley-Blackwell.
- Schuck, P., Piot, M., Méjean, S., Le Graet, Y., Fauquant, J., Brulé, G., et al. (1994). Déshydratation par atomisation de phosphocaseinate natif obtenu par microfiltration sur membrane. *Le Lait*, 74(5), 375–388.
- Silva, N. N., Piot, M., de Carvalho, A. F., Violleau, F., Fameau, A.-L., et al. (2013). pH-induced demineralization of casein micelles modifies their physico-chemical and foaming properties. *Food Hydrocolloids*, 32(2), 322–330.
- Silva, N. N., Saint-Jalmes, A., de Carvalho, A. F., & Gaucheron, F. (2014). Development of casein microgels from cross-linking of casein micelles by genipin. *Langmuir*, 30(34), 10167–10175.
- Srinivasan, M., Singh, H., & Munro, P. A. (2001). Creaming stability of oil-in-water emulsions formed with sodium and calcium caseinates. *Journal of Food Science*, 66(3), 441–446.
- Trejo, R., Dokland, T., Jurat-Fuentes, J., & Harte, F. (2011). Cryo-transmission electron tomography of native casein micelles from bovine milk. *Journal of Dairy Science*, 94(12), 5770–5775.
- Udabage, P., McKinnon, I. R., & Augustin, M. A. (2001). Effects of mineral salts and calcium chelating agents on the gelation of renneted skim milk. *Journal of Dairy Science*, 84(7), 1569–1575.
- Vujicic, I., deMan, J. M., & Woodrow, I. L. (1968). Interaction of polyphosphates and citrate with skim milk proteins. *Canadian Institute of Food Technology Journal*, 1(1), 17–21.
- Walstra, P. (1990). On the stability of casein micelles. *Journal of Dairy Science*, 73(8), 1965–1979.
- Xu, Y., Liu, D., Yang, H., Zhang, J., Liu, X., Regenstien, J. M., et al. (2016). Effect of calcium sequestration by ion-exchange treatment on the dissociation of casein micelles in model milk protein concentrates. *Food Hydrocolloids*, 60, 59–66.
- Ye, A. (2011). Functional properties of milk protein concentrates: Emulsifying properties, adsorption and stability of emulsions. *International Dairy Journal*, 21(1), 14–20.